EXPERIMENTAL INVESTIGATIONS INTO THE EFFECT OF STRONG WINDS ON WAVE OVERTOPPING AT A VERTICAL SEAWALL

Naoto Inagaki, Waseda University, richedge68green@toki.waseda.jp
Tomoya Shibayama, Waseda University, shibayama@waseda.jp
Kunihiko Ishibashi, Niigata University, isibasik@eng.niigata-u.ac.jp
Ryota Nakamura, Niigata University, r-nakamura@eng.niigata-u.ac.jp
Miguel Esteban, Waseda University, esteban.fagan@gmail.com

INTRODUCTION

Given the possible future intensification of tropical cyclones as a consequence of ongoing global warming, it is becoming increasingly important to consider the effect that stronger winds will have on nearshore wave dynamics. Despite the possible influence of wind on the characteristics of wave overtopping having been suggested decades ago (e.g. Iwagaki et al., 1966), to the authors' knowledge, not so many studies on wave dynamics have discussed this effect (e.g. Ward, 1998). Hence, the present study quantitatively analyses the overtopping of coastal structures under various types of waves and wind speeds, and will discuss the wind effects on elementary hydrodynamic processes such as wave breaking.

METHODOLOGY

Experiments using a 1/40 scale were performed at the hydrodynamics laboratory of Niigata University, Japan. A wind fan with an air duct was mounted on a wave flume (length 10 m, height 0.8 m, width 0.4 m). The water depth was fixed at 0.35 m. A flap-type wave-maker was located behind the air duct, which generated periodic waves of various steepness (H_0/L_0 of 0.0102 to 0.0371, see Table 1). Despite the relatively low surf similarity parameter ξ, all waves became plunging-like breakers before a vertical seawall situated at the other end of the flume (see Figure 1). Three wind speeds U were used, of 0 m/s (no wind), 6.84 m/s, and 10.04 m/s.

A PIV analysis followed the overtopping experiments to investigate the velocity field of the water mass. To investigate the mass transfer, the mass flow rate $\boldsymbol{m}$ for a given cross-section A was used, which is given by:

$$\boldsymbol{m} = \iint \boldsymbol{J}_m \cdot \boldsymbol{n}\, dA = \sum_A (\rho \boldsymbol{u})(\Delta x_1 \times \Delta x_2) \quad (1)$$

$\boldsymbol{J_m}$ represents the mass flux and $\boldsymbol{n}$ means the normal unit vector of the cross-section. Δx_1 and Δx_2 denote the size the PIV grid, which was perpendicular to the stream.

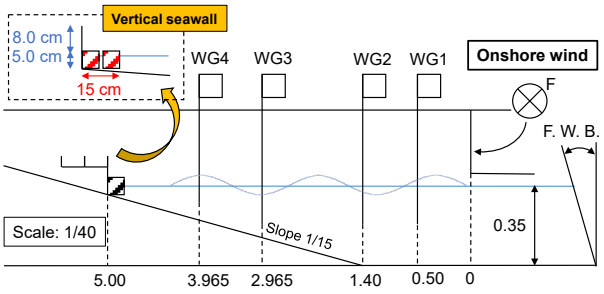

Figure 1. Schematic diagram of the experimental apparatus (not to scale).

Table 1. "Deepwater" parameters of waves generated by the wave-maker.

Wave height H_0 [m]	Wave period T_0 [s]	Wavelength L_0 [m]	Wave steepness H_0/L_0	Surf similarity parameter ξ [-]
0.0770	1.260	2.076	0.0371	0.327
0.0716	1.358	2.047	0.0350	0.337
0.0679	1.421	2.050	0.0331	0.346
0.0651	1.535	2.269	0.0287	0.372
0.0617	1.575	2.345	0.0263	0.388
0.0613	1.611	2.476	0.0248	0.400
0.0574	1.659	2.612	0.0220	0.425
0.0568	1.703	2.715	0.0209	0.435
0.0478	1.785	2.924	0.0163	0.493
0.0419	1.951	3.281	0.0128	0.557
0.0369	2.035	3.627	0.0102	0.624

RESULTS

The overtopping rate for each wave and wind speed is summarized in Figure 2, showing that in general the overtopping rate is significantly increased by the effect of the wind (see Figure 3). Although the stronger winds generally resulted in a higher overtopping rate, the high and low wave steepness (H_0/L_0 = 0.0371 and 0.0128) yielded higher overtopping rate for the U = 6.84 m/s case.

Accordingly, the PIV analysis focused on specific wave steepness such as 0.0220 (to clarify the mechanism of the maximum overtopping rate among the experiments), 0.0371 and 0.0128 (to investigate the reason for lower overtopping rate under stronger winds).

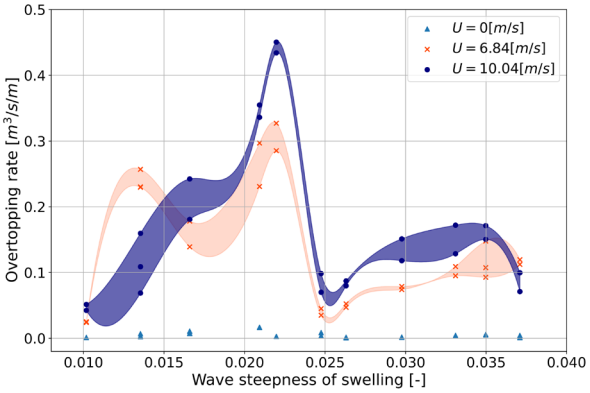

Figure 2. Overtopping rate for the different experimental cases (the values were corrected to real scale). At least 2 experiments were performed for each case to account for randomness in the overtopping rate. The curves show the envelopes connecting the maximum or the minimum value for each case.

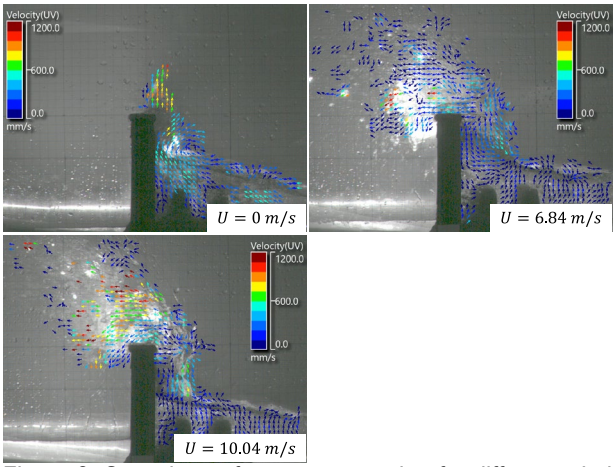

Figure 3. Snapshots of wave overtopping for different wind speed when H_0/L_0 = 0.0220.

The mass flow rate across two different imaginary lines (see Figure 4) was calculated by using the velocity field obtained from the PIV analysis (the results are shown in Table 2). Line A was set 10 mm under the crest of the vertical seawall, and Line B was perpendicular to the starting uppermost seaward point of the structure. A positive correlation was found between the mass flow rate and the overtopping rate shown in Figure 2. The variation of the mass flow rate between the two different wind speeds (6.84 m/s and 10.04 m/s) was around ±10-20 %, and was not linear.

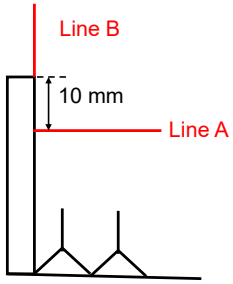

Figure 4. Schematic diagram of the intersection over which mass flow rate was calculated.

Table 2. Mass flow rate for specific wave steepness (at the experimental scale). See Figure 4 for the location of Lines A and B). Input speeds were 0 m/s (No), 6.84 m/s (Middle), and 10.04 m/s (High).

	$H_0/L_0 = 0.0128$			$H_0/L_0 = 0.0220$			$H_0/L_0 = 0.0371$		
	No	Middle	High	No	Middle	High	No	Middle	High
Line A (m_z)	13.485	41.173	26.850	13.786	29.197	32.273	11.961	21.806	15.814
Line B (m_x)	6.768	30.470	24.740	6.752	31.198	35.985	7.247	26.622	18.154

Unit: $kg \cdot s^{-1}/m$

DISCUSSION

The increase of the mass flow rate through Line A due to the effect of wind suggested that there was a certain lift-up effect of the wind along the wall. The mass flow rate through Line B provides an indication of the shoreward transfer of energy due to wind, including both lift-up and shoreward transfer (see Figure 3). It is worth mentioning that the mass flow rate estimated from the PIV measurements for the high wind case in Table 2 could be conservative, as this method cannot track small splash (which is more likely to occur under high winds).

For the case of the wave steepness 0.0220 (the maximum overtopping rate), it was found that a large amount of water mass was launched by a partially standing wave, and the wave breaking and resulting turbulence tended to be smaller than in the case with other wave steepnesses. In that sense, there appear to be some specific wave steepnesses that are particularly susceptible to result in large amplification of overtopping due to wind (see Figure 5, which shows the shoreward deformation of what would have been a standing wave under no wind condition. Some of this projected water particles will end up behind the structure, though others will land in front of it)

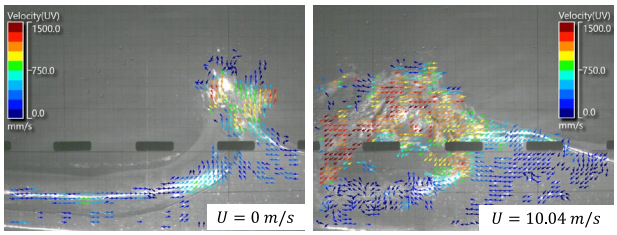

Figure 5. Launched volume during a partially standing wave, left) no wind, right) U= 10.04 m/s. The water mass was launched upward for the cases with no wind, though it was projected shoreward when wind forcing was present.

The presence of wind influenced breaker location and type. For the wave steepness of 0.0371, a strong onshore

wind initiated early wave breaking (at a deeper location), which was consistent with previous studies by Ward (1998) and González-Escrivá (2007) (see Figure 6). Early wave breaking would result in a more turbulent "bore" to travel a longer distance (hence more energy loss). For the wave steepness of 0.0128, a variation of a breaker type was clearly observed. The winds caused more-plunging-like breaker and hence more energy loss by larger turbulence than in the case with no wind (see Figure 7). This is not consistent with previous research, and for example Galloway et al. (1989) and Douglass (1990) suggested instead that stronger onshore wind would result in a more-spilling-like breaker. In the present experiment the variation of breaking type and location were found to cause more energy loss, which essentially accounts for the cases where the middle wind speed yielded more overtopping rate than the high wind speed (see H_0/L_0 of 0.0128 and 0.0371 in Figure 2).

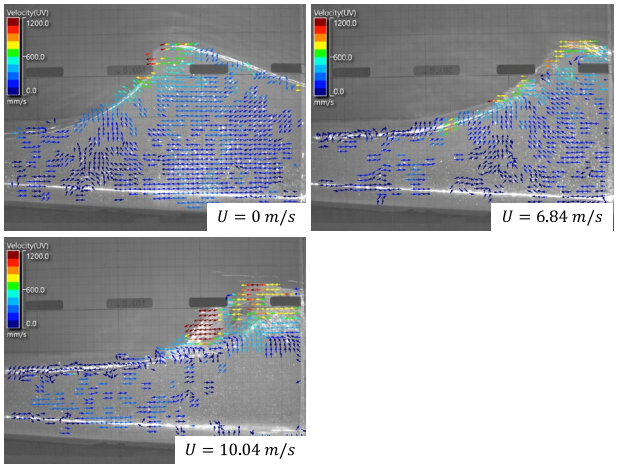

Figure 6. Snapshots of the plunging wave breaking for various wind speeds. The photos were taken from the same angle of view.

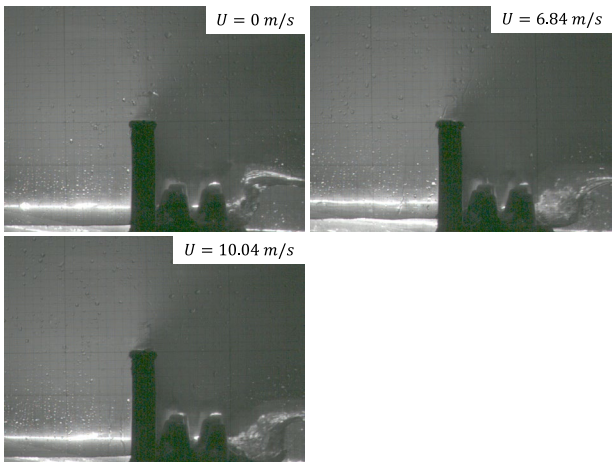

Figure 7. Snapshots of the breaker front for various wind speeds. A larger turbulent front was found for stronger winds.

CONCLUSIONS

Generally speaking, the overtopping rate over a coastal structure appears to be increased by stronger onshore wind speeds. The PIV analysis conducted revealed that wind could influence the mass flow rate and thus overtopping, through a certain lift-up effect and shoreward transport.

The potential mechanisms governing such increases in overtopping were investigated for a range of wave steepnesses. The variation of breaker location and type is influenced by wind, and this indirectly affects the overtopping rate (smaller overtopping rate with higher wind speeds).

Using the results of such laboratory experiments would make it possible in the future to improve the model developed by Inagaki et al. (2022), to better predict the energy dissipation process of breaking waves under wind and water mass transport due to strong winds.

REFERENCES

Douglass, S. L. (1990). Influence of wind on breaking waves. *Journal of Waterway, Port, Coastal and Ocean Engineering*, *116*(6), 651-663.

Galloway, J. S., Collins, M. B., & Moran, A. D. (1989). Onshore/offshore wind influence on breaking waves: An empirical study. *Coastal Engineering*, *13*, 305-323.

González-Escrivá, J. A. (2007). The role of wind in wave runup and overtopping of coastal structures. In *Coastal Engineering 2006* (pp. 4766-4778). World Scientific.

Inagaki, N., Shibayama, T., Takabatake, T., Esteban, M., Mäll, M., & Kyaw, T. O. (2022). Increase in overtopping rate caused by local gust-winds during the passage of a typhoon. *Coastal Engineering Journal*, 1-19.

Iwagaki, Y., Tsuchiya, Y., & Inoue, M. (1966). On the effect of wind on wave overtopping on vertical seawalls. *Bulletin Disaster Prevention Research Institute, Kyoto University*, *16*(1), 11-30.

Ward, D. L. (1998). *Wind effects on runup and overtopping of coastal structures*. Texas A&M University.